Journal of Power Sources 196 (2011) 8683–8687

Contents lists available at ScienceDirect

Journal of Power Sources

journal homepage: www.elsevier.com/locate/jpowsour

Short communication

Al-doped $Li_7La_3Zr_2O_{12}$ synthesized by a polymerized complex method

Ying Jin*, Paul J. McGinn

Department of Chemical and Biomolecular Engineering, University of Notre Dame, Notre Dame, IN 46556, USA

ARTICLE INFO

Article history:
Received 18 April 2011
Received in revised form 23 May 2011
Accepted 24 May 2011
Available online 31 May 2011

Keywords:
$Li_7La_3Zr_2O_{12}$
Pechini processing
Solid electrolyte

ABSTRACT

$Li_7La_3Zr_2O_{12}$ electrolytes doped with different amounts of Al (0, 0.2, 0.7, 1.2, and 2.5 wt.%) were prepared by a polymerized complex (Pechini) method. The influence of aluminum on the structure and conductivity of $Li_7La_3Zr_2O_{12}$ were investigated by X-ray diffraction (XRD), impedance spectroscopy, scanning electron microscopy (SEM), and thermal dilatometry. It was found that even a small amount of Al (e.g. 0.2 wt.%) added to $Li_7La_3Zr_2O_{12}$ can greatly accelerate densification during the sintering process. SEM micrographs showed the existence of a liquid phase introduced by Al additions which led to the enhanced sintering rate. The addition of Al also stabilized the higher conductivity cubic form of $Li_7La_3Zr_2O_{12}$ rather than the less conductive tetragonal form. The combination of these two beneficial effects of Al enabled greatly reduced sintering times for preparation of highly conductive $Li_7La_3Zr_2O_{12}$ electrolyte. With optimal additions of Al (e.g. 1.2 wt.%), $Li_7La_3Zr_2O_{12}$ electrolyte sintered at 1200 °C for only 6 h showed an ionic conductivity of 2.0×10^{-4} S cm^{-1} at room temperature.

1. Introduction

The application of lithium ion batteries for electric vehicles needs safe electrolyte materials with high lithium ion conductivity. The commonly used organic and polymer electrolytes have potential safety issues such as flammability, as well as operating temperature limitations. Solid electrolytes are considered an alternative to these common electrolytes. However, the conductivity of solid electrolytes is typically not as high as that exhibited by liquid electrolytes. After decades of research, the conductivity of several solid electrolyte materials is now approaching that of organic electrolytes [1–5]. Among the solid electrolytes, the so-called stuffed lithium garnet $Li_7La_3Zr_2O_{12}$, recently reported by Weppner's group [6], has attracted much attention due to its relatively high ionic conductivity (3×10^{-4} S cm^{-1} at 25 °C). It has been reported that this material has high chemical and electrochemical stability with lithium metal [7,8]. Members of the lithium garnets are the subject of a recent review by Cussen [9].

The garnet structure of $Li_7La_3Zr_2O_{12}$ has two symmetries: tetragonal and cubic [10,11]. The conductivity of the tetragonal phase is two orders of magnitude lower than the cubic phase [11]. To synthesize the more conductive cubic phase of $Li_7La_3Zr_2O_{12}$, long sintering at temperatures of 1200 °C and above has been thought to be the key factor controlling the transformation from tetragonal to cubic. Therefore, to obtain the highly conductive cubic phase, 36 h of sintering at or above 1200 °C was usually applied to synthesize this material [6–8,12,13]. Recently, Geiger et al. [14] reported that Al contamination from the crucible may be the key aspect in stabilizing the cubic phase, rather than the long sintering time. They suggested that Al might be introduced to the garnet crystal by a reaction between the molten precursors (Li_2CO_3 or LiOH) and the crucible wall during the heat treatment.

In order to find an improved synthesis process, it is important to know how Al affects the structure and conductivity of the $Li_7La_3Zr_2O_{12}$(LLZO) electrolyte. Thirty-six hours of sintering above 1200 °C could be a major obstacle for use of this solid electrolyte. In particular at these temperatures Li loss becomes a major concern. In the reported work to date, solid state processing has almost exclusively been used. In the conventional solid state synthesis method, repeated heat treatments and intermittent grinding are necessary to ensure the oxide precursors react thoroughly. The polymerized complex method (also referred to as the Pechini process) begins with liquid precursors, so provides molecular level mixing of the components [15]. The result is that precursors can react completely at lower temperatures and in shorter times, without the need for intermittent grinding, and this synthesis route typically yields finer powders with a more uniform size distribution [16–18]. In the present work, Pechini processing is applied to synthesize LLZO powders with different amounts of Al. The sintering of these powders was studied to investigate the influence of Al on processing, structure and conductivity of the LLZO electrolyte.

* Corresponding author at: 182 Fitzpatrick Hall, University of Notre Dame, Notre Dame, IN 46556-5637, USA. Tel.: +1 574 631 5692; fax: +1 574 631 8366.
E-mail address: yjin1@nd.edu (Y. Jin).

0378-7753/$ – see front matter © 2011 Elsevier B.V. All rights reserved.
doi:10.1016/j.jpowsour.2011.05.065

2. Experimental

2.1. Preparation of $Li_7La_3Zr_2O_{12}$

$LiNO_3$ anhydrous (99%), $La(NO_3)_3{\cdot}6H_2O$ (99.9%), $ZrOCl_2{\cdot}8H_2O$ (99.9%), and $Al(NO_3)_3{\cdot}9H_2O$ (98.0–102.0%), all purchased from Alfa Aesar, were used to prepare nitrate precursor solutions. The molar ratio between Li, La, and Zr was controlled as 7.7:3:2. Excess Li (10%) was added to compensate for expected Li loss during high temperature heat treatments. 0.2, 0.7, 1.2 and 2.5 wt.% of Al were added to $Li_7La_3Zr_2O_{12}$ by adding $Al(NO_3)_3{\cdot}9H_2O$ to the nitrate solution. These weight percents were based on the calculated $Li_7La_3Zr_2O_{12}$ product weight. Citric acid (99.5%, Aldrich) and ethylene glycol (Fisher Chemical), in the ratio of 60:40 mol were added to the nitrate solution as complexing agents. The overall metallic ion to organic ratio was 38:62 mol, which was used to achieve the desired foaming behavior without self-ignition followed by pyrolysis [16].

The organic solution was poured into the stirred nitrate solution. The mixture was heated at around 130 °C until a solidified white foam formed. The foam was crushed, and then calcined at 900 °C for 6 h (ramp rate: 5 °C min^{-1}) in air in an alumina crucible to react the precursors. After the calcination, the powder was pressed into a 1 cm diameter pellet in a uni-axial press (Carver Inc.) with a load of 40 MPa for 5 min. The pellet was sintered at 1200 °C in air for 6 h (ramp rate: 5 °C min^{-1}) on an alumina plate. A 2.4 cm diameter LLZO pellet made by conventional solid state method with no Al added was put between the small pellet and the alumina support plate to prevent interaction between the small sample pellet and the plate. The small pellet was covered by additional LLZO powder to reduce Li loss at high temperature. An alumina crucible was used to cover entire pellet assembly to help further reduce Li losses.

2.2. Characterization of $Li_7La_3Zr_2O_{12}$

The X-ray structural analysis of the $Li_7La_3Zr_2O_{12}$ powders was performed by powder diffractometry (Bruker powder X-ray diffractometer, CuKα, 40 kV, 40 mA) at room temperature. Sintered pellets were crushed to yield powder for XRD. Powder was extracted from the center region of the pellet to avoid near surface effects such as Li deficiency. The reference powder diffraction spectra of cubic and tetragonal LLZO were simulated from cif files [10,11].

The microstructures of the electrolyte pellets were observed by scanning electron microscopy (SEM) (EVO 50 Series, Zeiss). Before SEM observation, the sintered pellets were polished using diamond paste on a polishing wheel (MultiPrep, ALLIED high tech products Inc.) The composition distribution of the elements was measured in the SEM by energy dispersive X-ray spectroscopy (EDS) (INCAxsight Model 7636, Oxford Instruments).

Electrochemical impedance spectroscopy measurements were performed with an impedance analyzer (1260 Impedance/Gain-Phase analyzer, Solartron) combined with a dielectric interface (1296 Dielectric Interface, Solartron). Silver paint was applied on each side of the electrolyte pellet to make the current collector layers. Leads to the sample were made by attaching Cu wires to the painted ends. Impedance spectra were collected by sweeping the frequency from 13 MHz to 5 Hz with a voltage set at 10 mV. Ionic conductivity values were calculated from the complex impedance plots using ZView2 (Scribner Associates) for analysis. To test the electrolyte performance in a cell, cathode ($LiMn_2O_4$) and anode ($Li_4Ti_5O_{12}$) films were deposited on each side of a polished 0.5 mm thick 1.2 wt.% Al-doped LLZO slice. Pulsed laser deposition (PLD) was used to deposit the films, while the substrate was maintained at 200 °C. Post-deposition annealing in air at 400 °C for 5 min was applied to improve the films' crystallinity. Ag films were thermal evaporated on top of the electrode films as current collectors. A potentiostat (Voltalab PST050, Radiometer Analytical) was used to test the cell performance of the battery. The charging and discharging current density was 1 μA cm^{-2}.

High temperature dilatometry (L75, Linseis) was used to observe the sample shrinkage associated with sintering as a function of temperature. The pellet was ramped to 1250 °C at a rate of 10 °C min^{-1}.

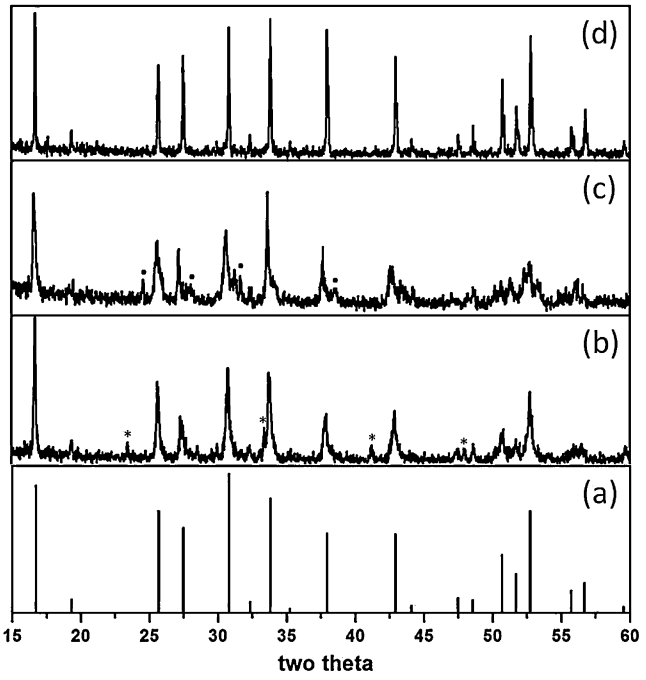

Fig. 1. XRD spectra of $Li_7La_3Zr_2O_{12}$ with 1.2 wt.% of Al after different steps during synthesis: (a) simulated pattern of cubic LLZO based on structure from Ref. [11], (b) LLZO calcined at 900 °C for 6 h, (c) LLZO sintered at 1200 °C for 1 h, and (d) LLZO sintered at 1200 °C for 6 h (*, $LaAlO_3$; ·, $La_2Li_{0.5}Al_{0.5}O_4$).

3. Results and discussion

3.1. XRD results

Fig. 1 shows the X-ray diffraction patterns of the $Li_7La_3Zr_2O_{12}$ powder with 1.2 wt.% added Al after different heat treatment steps. After the first heat treatment (calcination at 900 °C for 6 h), the major phase in this powder can be determined as cubic LLZO, which indicates the precursors have reacted completely with each other in this calcination process. $LaAlO_3$ appears as a second phase in this powder (corresponding peaks denoted by asterisks in Fig. 1(b)). The second step of heat treatments is sintering at 1200 °C. Fig. 1(c and d) shows the patterns for LLZO sintered at 1200 °C for 1 h and 6 h, respectively. Comparing with the pattern in Fig. 1(b), after 1-h sintering at 1200 °C, the peaks from impurity phase shift, indicating a new phase formed. The peaks from the new impurity phase match well with the pattern of lanthanum lithium aluminum oxide ($La_2Li_{0.5}Al_{0.5}O_4$). This phase could be formed by the reaction between $LaAlO_3$ and the Li in the LLZO at 1200 °C. As the sintering time increased to 6 h, the XRD pattern shows the powder is well crystallized cubic LLZO, with any Al-containing second phase being below the detection limit. The absence of Al-containing impurity phase in this XRD pattern is likely the result of more complete reaction with LLZO during the 6-h sintering, resulting in an Al-doped $Li_7La_3Zr_2O_{12}$.

Fig. 2 shows XRD patterns of LLZO electrolytes sintered at 1200 °C for 6 h with different amounts of added Al. Without adding Al, the LLZO sintered at 1200 °C for 6 h can be determined as a mixture of tetragonal LLZO, La_2O_3, and $La_{0.5}Zr_{0.5}O_{1.75}$ (Fig. 2(b)). After the addition of Al, even as low as 0.2 wt.%, the tetragonal LLZO phase

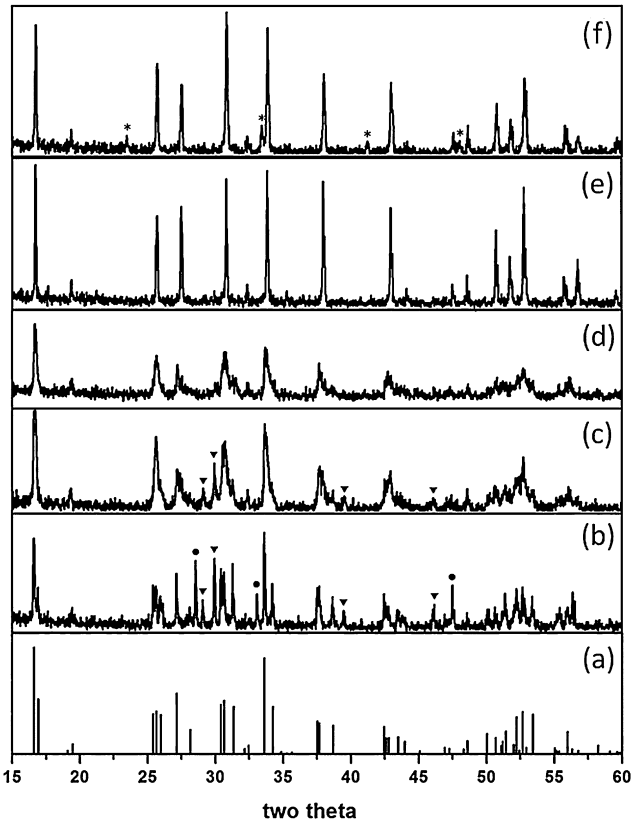

Fig. 2. (a) Simulated pattern of tetragonal $Li_7La_3Zr_2O_{12}$ based on structure from Ref. [10], (b) undoped LLZO sintered at 1200 °C for 6 h (▼, La_2O_3; ●, $La_{0.5}Zr_{0.5}O_{1.75}$), (c) 0.2 wt.% Al doped LLZO sintered at 1200 °C for 6 h (▼, La_2O_3), (d) 0.7 wt.% Al doped LLZO sintered at 1200 °C for 6 h, (e) 1.2 wt.% Al doped LLZO sintered at 1200 °C for 6 h, and (f) 2.5 wt.% Al doped LLZO sintered at 1200 °C for 6 h (*, $LaAlO_3$).

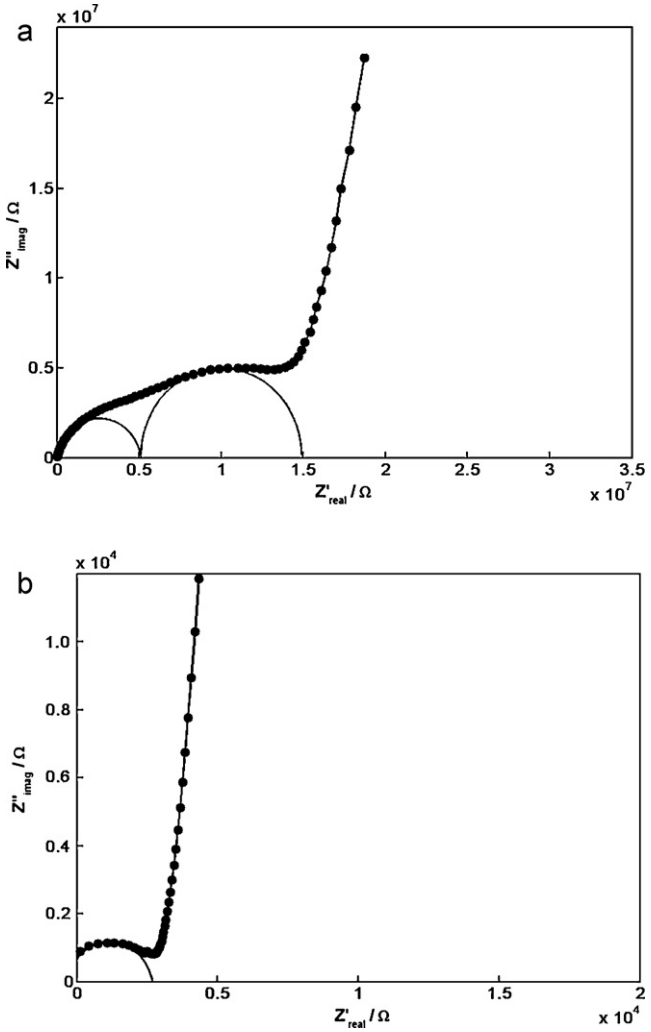

Fig. 3. (a) Impedance spectra of the 0 wt.% Al $Li_7La_3Zr_2O_{12}$ electrolyte (frequency range: 13 MHz–5 Hz.) (thickness (mm) of the pellet: 5.4; diameter (mm): 10.46; estimated R (Ohms) of the small circle at high frequency part: 5.118×10^6), (b) impedance spectra of the 1.2 wt.% Al $Li_7La_3Zr_2O_{12}$ electrolyte (high frequency part: 13 MHz–4.5×10^4 Hz) (thickness (mm) of the pellet: 3.2; diameter (mm): 8.26; estimated R (Ω): 3031).

is partially transformed to cubic LLZO. When the Al content is low (0.2 and 0.7 wt.%), the peaks from cubic LLZO are broad and have shoulders (Fig. 2(c and d)). The shoulder peaks are diffracted from tetragonal phase LLZO. Therefore, the LLZO with low content of Al is a mixture of cubic and tetragonal phases. As the Al content increases to 1.2 wt.%, the broad peaks become sharp, indicating the formation of a well crystallized cubic LLZO phase (Fig. 2(e), the same picture as Fig. 1(d)) without residual tetragonal LLZO. Impurity phases, such as La_2O_3, and $La_{0.5}Zr_{0.5}O_{1.75}$, gradually disappear with the increasing of Al addition.

By continuing to add Al to the level of 2.5 wt.% (Fig. 2(f)), in addition to the cubic LLZO phase, a new impurity phase, $LaAlO_3$, appears in the XRD pattern (peaks from this phase are marked by asterisks in Fig. 2(f)). The presence of $LaAlO_3$ suggests the 2.5 wt.% value exceeds the optimized doping value of Al in LLZO, with excess Al appearing in the form of $LaAlO_3$. However, the impedance measurements show that this impurity phase does not greatly affect the electrolyte conductivity at this level.

Since the sintering time for all the pellets are the same, the transition of LLZO tetragonal to cubic in Fig. 2 is due to the varying Al doping level. Geiger et al. [14] suggest that Al atoms occupy a Li site in the garnet structure and stabilize the cubic phase at room temperature. The XRD data verify that the addition of Al promotes the transformation of LLZO from the tetragonal phase to the cubic phase.

3.2. Impedance measurement

Table 1 summarizes the density and lithium ion conductivity of the LLZO pellets with different Al contents sintered at 1200 °C for 6 h. Density measurements were simply preformed by weighting the pellets' mass and measuring their diameter and height. The pellet without Al has a very low density compared to the theoretical value (5.098 g cm^{-3} [11]). Particles are not well bonded to each other as they can easily be scraped off from the pellet. The impedance spectrum (Fig. 3(a)) of this pellet shows a grain boundary semicircle in the middle frequency range which is likely caused by these poorly joined particles. The high frequency semicircle is from the bulk LLZO electrolyte. The impedance spectra of all the other Al-doped $Li_7La_3Zr_2O_{12}$ samples have only one semicircle in the high frequency range and a line in the low frequency range due to the Li blocking electrodes.

The density of the $Li_7La_3Zr_2O_{12}$ pellets jumps from 2.6 to 4.4 g cm^{-3} by adding Al and does not change significantly with variations in the Al content. The conductivity of the LLZO pellets increases with Al content up to ~1.2 wt.% showing the beneficial effect of Al additions. However, when the amount of Al increases to 2.5 wt.%, the Al in the LLZO is saturated and an impurity phase ($LaAlO_3$) forms at levels detected by XRD, which may cause the slightly reduced conductivity of this pellet.

Table 1
Density and conductivity of LLZO pellets with different Al contents, sintered at 1200 °C for 6 h.

	No Al added	0.2 wt.% Al	0.7 wt.% Al	1.2 wt.% Al	2.5 wt.% Al
Mass density ($g\,cm^{-3}$)	2.6	4.4	4.5	4.4	4.5
25 °C Li^+ conductivity ($S\,cm^{-1}$)	1.2×10^{-7}	2.2×10^{-5}	3.5×10^{-5}	2.0×10^{-4}	1.96×10^{-4}

3.3. Al microstructure effects

The effect of Al additions on LLZO sintering was investigated through dilatometry and microstructure observations. A dilatometer was used to measure the change of length of a 1.2 wt.% Al-doped LLZO pellet during heating to 1250 °C. An onset temperature for pronounced shrinkage was found at 1052 °C. Based on the sudden dimension change observed in the dilatometer, the sintering appears to be enhanced by the presence of a liquid phase.

To confirm the sintering mechanism in Al-doped LLZO, two pellets (0.2 and 1.2 wt.% Al) were sintered at 1200 °C for 1 h and quenched to room temperature prior to observation. The densities of these two pellets were: 4.3 $g\,cm^{-3}$ (0.2 Al) and4.6 $g\,cm^{-3}$ (1.2 Al). These density values are close to those of the 6-h sintered pellets, indicating that densification of the pellets occurs relatively quickly. However, the conductivities of the pellets (9.5×10^{-6} and 4.2×10^{-5} $S\,cm^{-1}$, respectively) are not as high as the pellets sintered 6-h, suggesting that sintering occurs more rapidly than establishment of the optimal Al-stabilized crystallographic structure.

SEM observations (Fig. 4) shows the presence of a second phase (distinguished by the lighter shade of grey in Fig. 4) in both of the pellets. The second phase exists at the intersection of the particles and appears like a liquid wetting particle surfaces. The evidence suggests this phase plays the role of a liquid phase during sintering of LLZO resulting in accelerated pellet densification. During liquid phase sintering, when the temperature reaches the melting point of the liquid phase, wetting of particle surfaces by the liquid phase results in capillary forces that facilitate particle rearrangement and enhanced diffusion that accelerates densification [19].

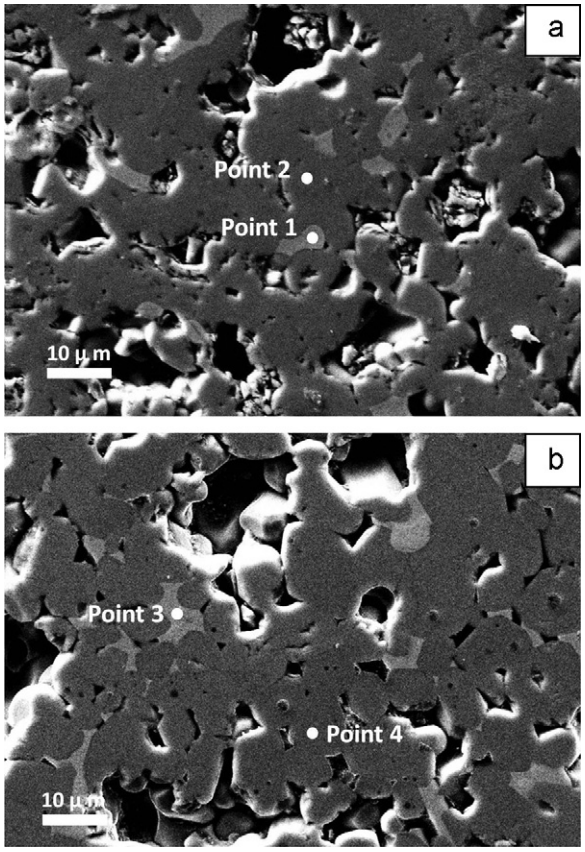

Fig. 4. SEM picture of microstructures (a) 0.2 wt.% Al $Li_7La_3Zr_2O_{12}$ pellet sintered at 1200 °C for 1 h, and (b) 1.2 wt.% Al $Li_7La_3Zr_2O_{12}$ pellet sintered at 1200 °C for 1 h. The magnification of all the pictures are 4k×.

Significant porosity is evident in the microstructures, some of which may result from the polishing process (e.g. pull outs during polishing). Compositions of the matrix phase and the minority phases were characterized by EDS, and are summarized in Table 2. Comparing the composition differences between them, the Al and La levels are higher in the minority phase (points 1 and 3) while the Zr content is lower. Based on the XRD pattern in Fig. 1(c) shows, it is likely that the second phase in the 1.2 wt.% Al doped LLZO (Fig. 4 (b)) is $La_2Li_{0.5}Al_{0.5}O_4$. However, the exact composition of this phase is not known as Li cannot be detected by EDS, and matrix effects, due to the X-ray penetration depth in EDS, can also affect the apparent composition.

The formation of a liquid phase during sintering may initially occur by a reaction between Li_2O and Al_2O_3. The phase diagram shows a eutectic liquid forms at 23 mol% Al_2O_3 that has a melting point of 1055 °C [20], which corresponds well with the 1052 °C shrinkage onset temperature observed by dilatometry. During sintering, dissolution and reprecipitation will occur in the presence of the liquid which likely results in incorporation of La and Zr in the liquid.

It appears that Al additions to LLZO play two significant roles. As suggested by Weppner and co-workers [14], small amounts of Al appear to stabilize the cubic structure relative to the tetragonal structure. Secondly, from a processing standpoint the liquid phase that develops as a result of Al additions serves to promote densification and shorten sintering times. In typical solid state processing in alumina crucibles, some Al incorporation occurs through interactions with the crucible. However, this is typically insufficient to promote either significant densification or stabilization of the cubic structure, so very long sintering times are needed at high temperatures [6–8,12,13]. It is not clear what the optimal level of Al incorporation in LLZO is for cubic structure stabilization. Some amount in excess of this level is need for liquid phase sintering, as the liquid does not appear to be transient, so some Al remains behind along grain boundaries in the frozen liquid. There is also an optimal liquid content so as to sufficiently promote rapid sintering without reducing LLZO grain to grain contact too much. If an excessive amount of liquid forms, the pockets of liquid will reduce the grain boundary area available for Li-ion conduction.

Reducing the processing time needed at elevated temperature is important in limiting the extent of Li loss. The enhanced densification rate provided by the liquid is significant, for reasonably dense pellets can be processed in much shorter sintering time. Development of a liquid will also accelerate the cubic LLZO formation

Table 2
EDS result of the points in the SEM pictures (all results in atomic %).

	Al	Zr	La	O
Point 1	0.5	0.9	36.0	62.6
Point 2	0.2	11.6	16.5	71.7
Point 3	2.4	4.6	26.1	66.9
Point 4	0.1	10.4	14.7	74.8

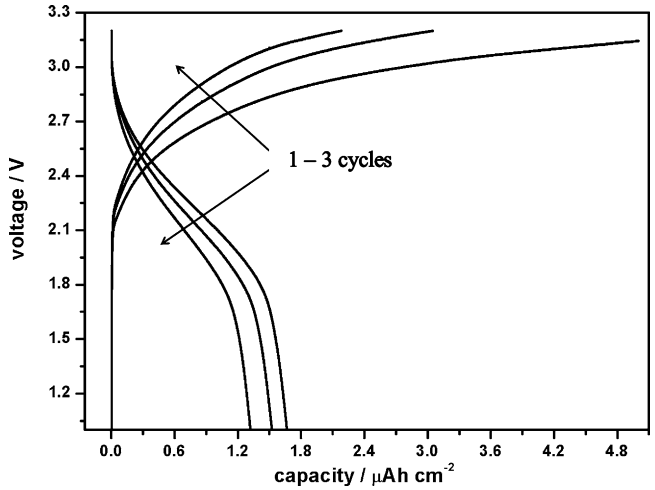

Fig. 5. Charging and discharging profile of a $LiMn_2O_4$/Al-doped LLZO/$Li_4Ti_5O_{12}$ cell at the current density of 1 $\mu A\,cm^{-2}$.

through enhanced diffusion. The polymerized complex method is also beneficial in this regard as it produces finer particles than solid state processing.

What remains to be clarified is the minimum residence time at high temperature for incorporation of Al into the LLZO lattice and stabilization of the cubic structure. The mixed phase structures (cubic and tetragonal) seen in Fig. 1 suggest this may be the process time determining factor.

3.4. Cell performance

To verify the feasibility of using LLZO as the electrolyte in solid state lithium ion batteries, $LiMn_2O_4$ and $Li_4Ti_5O_{12}$ films were deposited on each side of a polished 1.2 wt.% Al-doped LLZO slice by PLD. Fig. 5 shows the charging and discharging behavior of the battery at the current density of 1 $\mu A\,cm^{-2}$. The battery could be successfully cycled in the expected voltage range of (1.0–3.2 V). The low charge and discharge capacity result from the low mass of the PLD films (~0.5 μm thickness for both electrode films). In each cycle, an irreversible capacity could be observed. It is likely that this low coulombic efficiency (increased from 30% to 60% after 3 cycles) is due to the internal and interfacial resistance of this battery. Thinner and better polished electrolyte slices will be prepared in the future to fabricate improved solid state lithium ion batteries. The lack of an obvious discharging plateau (should be at ~2.5 V) could be caused by the low crystallinity of the electrode films deposited by PLD. An optimized post-annealing treatment, to ensure complete crystallization of the electrode films while avoiding deleterious interactions with the electrolyte, is needed for enhanced cell performance.

4. Conclusions

$Li_7La_3Zr_2O_{12}$ electrolytes with various Al contents (0, 0.2, 0.7, 1.2, and 2.5 wt.%) were prepared by the polymerized complex method. It was observed that the phase transformation from tetragonal to cubic occurred most readily when a certain level of Al was added to $Li_7La_3Zr_2O_{12}$. Moreover, even small amounts of Al (e.g. 0.2 wt.%) can greatly increase the density of $Li_7La_3Zr_2O_{12}$ pellets after sintering. SEM observations of Al-doped pellets verified the existence of a liquid phase. Dilatometry showed pellet densification accelerated around 1055 °C suggestive of formation of a Li_2O–Al_2O_3 eutectic. By addition of a proper amount of Al the synthesis of highly ionic conductive cubic $Li_7La_3Zr_2O_{12}$ can be greatly simplified. 1.2 wt.% Al-doped $Li_7La_3Zr_2O_{12}$ with $2 \times 10^{-4}\,S\,cm^{-1}$ conductivity at room temperature was prepared with 6 h of sintering at 1200 °C. Cell performance of the $LiMn_2O_4$/Al-doped LLZO/$Li_4Ti_5O_{12}$ battery shows that $Li_7La_3Zr_2O_{12}$ is a prospective electrolyte material in solid state lithium ion batteries.

Acknowledgements

The authors wish to thank Dr. JunjiAwaka for graciously providing cif files for the cubic and tetragonal forms of LLZO. This material is based upon work supported by the U.S. Army TARDEC under Contract No. W56HZV-08-C-0236, through a subcontract with Mississippi State University, and was performed for the simulation Based Reliability and Safety (SimBRS) research program. Any opinions, findings and conclusions or recommendations expressed in this material are those of the author(s) and do not necessarily reflect the views of the U.S. Army TARDEC.

References

[1] J.M. Kim, G.B. Park, K.C. Lee, H.Y. Park, S.C. Nam, S.W. Song, J. Power Sources 189 (2009) 211–216.
[2] P. Knauth, Solid State Ionics 180 (2009) 911–916.
[3] J.W. Fergus, J. Power Sources 195 (2010) 4554–4569.
[4] J. Fu, Solid State Ionics 96 (1997) 195–200.
[5] A.D. Robertson, A.R. West, A.G. Ritchie, Solid State Ionics 104 (1997) 1–11.
[6] R. Murugan, V. Thangadurai, W. Weppner, Angew. Chem. Int. Ed. 46 (2007) 7778–7781.
[7] A. Kaeriyama, H. Munakata, K. Kajihara, K. Kanamura, Y. Sato, T. Yoshida, ECS Trans. 16 (24) (2009) 175–180.
[8] M. Kotobuki, H. Munakata, K. Kanamura, Y. Sato, T. Yoshida, J. Electrochem. Soc. 157 (10) (2010) A1076–A1079.
[9] E.J. Cussen, J. Mater. Chem. 20 (2010) 5167–5173.
[10] J. Awaka, N. Kijima, H. Hayakawa, J. Akimoto, J. Solid State Chem. 182 (2009) 2046–2052.
[11] J. Awaka, A. Takashima, K. Kataoka, N. Kijima, Y. Idemoto, J. Akimoto, Chem. Lett. 40 (2011) 60–62.
[12] K.H. Kim, Y. Iriyama, K. Yamamoto, S. Kumazaki, T. Asaka, K. Tanabe, C.A.J. Fisher, T. Hirayama, R. Murugan, Z. Ogumi, J. Power Sources 196 (2011) 764–767.
[13] S. Ohta, T. Kobayashi, T. Asaoka, J. Power Sources 196 (2011) 3342–3345.
[14] C. Geiger, E. Alekseev, B. Lazic, M. Fisch, T. Armbruster, R. Langner, M. Fechtelkord, N. Kim, T. Pettke, W. Weppner, Inorg. Chem. 50 (2011) 1089–1097.
[15] M. Kakihana, J. Ceram. Soc. Jpn. 117 (2009) 857–862.
[16] H.M. Reichenbach, P.J. McGinn, J. Mater. Res. 16 (4) (2001) 967–974.
[17] Y.X. Gao, X.P. Wang, W.G. Wang, Z. Zhuang, D.M. Zhang, Q.F. Fang, Solid State Ionics 181 (2010) 1415–1419.
[18] E.N.S. Muccillo, R.A. Rocha, R. Muccillo, Mater. Lett. 53 (2002) 353–358.
[19] R.M. German, P. Suri, S.J. Park, J. Mater. Sci. 44 (2009) 1–39.
[20] L.P. Cook, E.R. Plante, Ceram. Trans. 27 (1992) 193–222.